



This open access document is published as a preprint in the Beilstein Archives with doi: 10.3762/bxiv.2019.153.v1 and is considered to be an early communication for feedback before peer review. Before citing this document, please check if a final, peer-reviewed version has been published in the Beilstein Journal of Organic Chemistry.

This document is not formatted, has not undergone copyediting or typesetting, and may contain errors, unsubstantiated scientific claims or preliminary data.

Preprint Title Identification of a novel binding mechanism of quinoline based molecules with lactate dehydrogenase of *Plasmodium falciparum*

Authors Rahul Singh, Vijay Bhardwaj and Rituraj Purohit

Publication Date 06 Dez 2019

Article Type Full Research Paper

Supporting Information File 1 Scanned Document.pdf; 822.2 KB

ORCID® IDs Rituraj Purohit - <https://orcid.org/0000-0002-2101-9398>

Identification of a novel binding mechanism of quinoline based molecules with lactate dehydrogenase of *Plasmodium falciparum*.

Rahul Singh^{1,2}, Vijay Bhardwaj^{1,2}, Rituraj Purohit^{*1, 2, 3}

¹Structural Bioinformatics Lab, CSIR-Institute of Himalayan Bioresource Technology (CSIR-IHBT), Palampur, HP, 176061, India

²Biotechnology division, CSIR-IHBT, Palampur, HP, 176061, India

³Academy of Scientific & Innovative Research (AcSIR), CSIR-IHBT Campus, Palampur, HP, 176061, India

*Author for correspondence (rituraj@ihbt.res.in)

Abstract

Malaria remains a deadliest disease brought about by Plasmodium species, among one of these species, disease due to *Plasmodium falciparum* (*Pf*) is life-threatening. The structures of *Pf*LDH and human LDH are very similar in terms of L-LDH activity, and their biological functions are also equivalent. Therefore, any treatment aiming blocking the functions of *Pf*LDH can affect human LDH. Thus, the main objective of this study is to identify the molecule that exhibits selectivity towards *Pf*LDH without a profound effect on human LDH. In this research, a set of 68 quinolines based molecules were used for molecular docking. From molecular docking, we selected molecules 3j, 4b, 4h, 4m based on their binding affinity, ligand efficiency, lipophilic ligand efficiency, and torsion with selectivity towards *Pf*LDH. The stability of the docked molecules was compared to Chloroquine (reference inhibitor) by applying molecular dynamics simulations and molecular mechanics poisson boltzmann surface area calculations. All the selected molecules showed selectivity for *Pf*LDH with stable dynamic behavior and high binding free energy in comparison to Chloroquine. After examining the molecular mechanics poisson boltzmann surface area ratio results, molecule 3j was reported as a potential and specific inhibitor for *Pf*LDH with a novel mechanism of binding to *Pf*LDH while the remaining molecules 4b, 4h, 4m could further be modified to be used as potent inhibitors against malarial infection.

Keywords: *Pf*LDH; MM-PBSA; molecular docking; MD simulations; LE; LLE.

Introduction

Malaria remains a deadliest disease brought about by Plasmodium species, among one of these species, sickness due to *Plasmodium falciparum* (*Pf*) is life-threatening [1]. Health consequences of malaria have identified by the World Health Organisation (WHO) in 2017 [2] and evaluated that there were 219 million instances of malaria around the world. The gradual increase in drug resistance over *Pf* malaria has increased the malarial cases and associated deaths. This leads researchers to work on different targets of *Pf* to introduce drugs that are effective against *Pf* and other four malaria species that affect humans (*Plasmodium malariae*, *Plasmodium vivax*, *Plasmodium ovale*, and *Plasmodium knowlesi*) [3].

Chloroquine (CQ) has been utilized enormously as an antimalarial drug due to its capacity to treat malaria in addition to its reasonable cost. The tremendous achievement of CQ and its overwhelming use eventually led to its resistance in *Pf* and *Plasmodium vivax*. These two parasite species are responsible for most human malaria cases [4]. CQ resistance was first announced in both South America and Southeast Asia in the late 1950s. Since then, CQ-resistant strains have spread throughout the ranges where the conditions are suitable for the advancement of the parasite, particularly in the districts of sub-Saharan Africa [5, 6]. High paces of therapeutic failure and a couple of adverse impacts of drug CQ have been accounted for globally, of which the most serious are retinopathy, myopathy, neuromyopathy, and cardiomyopathy [7]. Extended treatment may cause retinal toxicity, decreased visual sharpness, diplopia, and respective loss of vision. The most well-known side effect is ominous responses of the gastrointestinal tract, barring seizures, sleep deprivation, and paresthesia; there are also reports of ototoxicity, shivering, itching, and change in skin color [7]. This has raised the requirement for the development of a new antimalarial drug that would be more effective in controlling malaria. Today, almost all countries have reported the presence of CQ-resistant strains [8]. Hence, an urgent need has emerged for the development of new drugs and insecticides that will help in controlling malaria.

There are various targets available for anti-malarial drugs such as plasmepsin I, plasmepsin II, plasmepsin V, falcipain 2, *Pf* lactate dehydrogenase (LDH), pyridoxal kinase. Among these targets (LDH) is a preferable target for anti-malarial drugs because it controls the production of adenosine triphosphate (ATP) in plasmodium via glycolytic pathway, and has unique amino acids at the active site as compared to other LDHs. Glycolytic pathways and related enzymes are thought to be vital drug targets due to their parasitic dependency on the glycolysis cycle for energy production [9, 10]. *Pf*LDH protein plays an essential role in the last step of glycolysis and catalyzes the inter-

conversion of pyruvate to lactate [9, 10]. The enzyme LDH is further associated with the development of NAD⁺, which is required for the glycolytic enzyme glyceraldehyde-3-phosphate dehydrogenase [10]. *Pf* parasites rely upon this enzyme for their energy production, which necessary for biochemical functioning, growth, and development. Thus, this enzyme is believed to be a significant drug target in malaria treatment. Inhibition of this enzyme activity brings about the death of the parasite. The sequence of amino acids for human LDH and *Pf*LDH shows less similarity, but their molecular and biological functions are similar in terms of L-LDH activity [11]. So that, the selective targeting of this significant glycolytic enzyme in *Pf*LDH may not disturb the human LDH [13]. These features recommend *Pf*LDH as an appropriate target for the structure-based design of novel antimalarials [11–13].

In this study, a set of 68 quinolines based synthetic molecules were used, which may not show resistance, as shown by CQ. CQ is assigned as a reference inhibitor to compare with the set of molecules to be tested for their inhibition and anti-resistant potential against *Pf*LDH.

This research was designed to identify the best selective inhibitor against the crystal structure of *Pf*LDH, which has no effect on human LDH. The second one was to rank and compare the selected molecules based on their selectivity for *Pf*LDH in comparison to FDA approved anti-malarial drug CQ. The last one to observe and differentiate the molecular mechanics-poisson boltzmann surface area (MM-PBSA) profiles of top-ranked molecules in comparison with CQ.

The molecular docking approach was used to understand the protein-ligand interactions and inhibition potential in terms of binding affinity and molecular dynamics (MD) simulations studies were carried out to attain the dynamic behavior and stability of the complexes. After MD simulations studies, the MM-PBSA method was employed to interpret the binding free energy.

Materials and Methods

Protein-Ligand selection

Crystallographic PDB structure of *Pf*LDH (PDB ID: 1LDG) and Human LDH (PDB ID: 1I10), the reference molecule CQ was retrieved from RCSB protein data bank [14], and a set of 68 in house synthesized quinolines molecules [15] were used depicted in Figure S1.

Docking Analysis

In silico docking, experiments were performed with the SeeSAR v9.2. Docking was performed for the active site of the *Pf*LDH and human LDH. The hydrogen dehydration (HYDE) scoring function used to calculate binding affinity after docking [16, 17] equation (1) implemented in SeeSAR [18]. The estimated affinity of binding visualized in SeeSAR ranges from mM < μ M < nM < pM. The selection of the top poses based on their visual HYDE scores while also considering the Lipophilic Ligand Efficiency (LLE), Ligand Efficiency (LE) and Torsion [19] contributions to binding for protein-ligand.

$$\Delta G_{Hyde} = \sum_{atom\ i} [\Delta G^i_{Dehyd^n} + \Delta G^i_{h-bonds}] \dots \dots \dots (1)$$

The HYDE scoring function depends on desolvation and hydration (atom type-specific) that have been conventionally associated with Octanol-water Partition Coefficients (Kow) of small molecules. In the binding process, the water particles around the ligand are removed, and those in the binding pocket of the protein are pressed out by the ligand. The hydrogen bonds of the protein-ligand to water particles are broken, which prompts a disfavored enthalpic contribution, although the mass discharge of water atoms. New hydrogen bonds built up between the protein and ligand may offset this energy loss. Additionally, hydrophobic interactions of protein-ligand in contact with water atoms lead to the brokenness in the water hydrogen bond network and show unfavorable energy. The removal of these water atoms from the hydrophobic surfaces and their discharge to the mass water initiates an increase in energy, called hydrophobic impact [16, 17].

The LLE a drug-like multi-parameter approach that merges lipophilicity and in vitro strength (pKi) of a drug candidate [20].

To determine the binding affinity of a ligand in association with the number of non-hydrogen atoms was conferred by Kuntz et al. [21]. Addition of their genuine idea of LE numerically described as the quotient of ΔG and the number of non-hydrogen atoms of the compound [22].

$$LE = \Delta G / N \dots \dots \dots (2)$$

$$\Delta G = -RT \ln K_i, N = \text{number of non-hydrogen atoms.}$$

Discovery Studio visualizer used to visualize 3D and 2D interactions [23]. Sequence identity search by using UCSF Chimera v1.13.1 [24].

MD- Simulations and MM-PBSA Analysis

MD-simulations were performed to check the binding stability of the topmost SeeSAR docked complexes *Pf*LDH and human LDH with molecules 3j, 4m, 4b, 4h along the CQ, executed in GROMACS 5.0.4 module [25]. There is a number of articles reported where MD-simulations have been applied as the tool to study the stability, functionality, and interactions of the protein-ligand complexes [26, 27]. Protein molecules topologies were produced by GROMACS 5.0.4, and ligands parameter and topology file were generated with the PRODRG server [28]. Subsequently, a production run of 250ns was executed for the receptor-ligand complexes. Examine the receptor-ligand dynamic interactions, and binding free energy calculations were performed by using the MM-PBSA method in *g_mmpbsa* utility of GROMACS [29]. The binding free energy was calculated as the aggregate of molecular mechanics potential energy (Electrostatic + Van der Waal), Solvent Accessible Surface Area (SASA), and solvation energy (polar + non-polar). MM-PBSA calculations were executed at default parameters. The Method can be defined by the calculations of the free energy, according to the following equations:

$$\Delta G_{\text{bind}} = G_{\text{complex}} - (G_{\text{rec}}^{\text{P}} + G_{\text{lig}}) \dots\dots\dots(1)$$

where, G_{complex} = total binding free energy of complex, $G_{\text{rec}}^{\text{P}}$ = free receptor, G_{lig} = unbound ligand.

$$G_x = E_{\text{MM}} + G_{\text{solv.}}^{\text{n}} \dots\dots\dots(2)$$

$G_x = G_{\text{complex}}$, G_{protein} or $G_{\text{lig.}}$, E_{MM} = Average energy of molecular mechanics, $G_{\text{solv.}}^{\text{n}}$ = free solvation energy.

$$E_{\text{MM}} = E_{\text{bond}} + E_{\text{non-bond}} (E_{\text{elec}} + E_{\text{vdW}}) \dots\dots\dots(3)$$

E_{bond} is always zero, and $E_{\text{non-bond}}$ includes electrostatic and Van der Waal interactions.

$$G_{\text{solv.}} = G_{\text{polar}} + G_{\text{non-polar}} \dots\dots\dots(4)$$

$G_{\text{solv.}}$ is calculated by equation (4) polar energy calculated by Poisson-Boltzmann equation and non-polar by SASA as given in the below equation :

$$G_{\text{non-polar}} = \gamma A + b \dots\dots\dots(5)$$

Where, γ = Surface tension co-efficient of the solvent, A as SASA, and b is fitting parameter [30].

Results and Discussion





















Structural similarity

The biological function of proteins depends primarily on their structure and folding dynamics. We found only a 28.16% sequence identity between human LDH and *Pf*LDH structures by the UCSF chimera tool. However, both the proteins share a similar 3D structure with a root mean square deviation of 1.062Å, as shown in Figure S2. Despite the low sequence similarity, both the proteins have a similar structure, which accounts for their coherence in molecular and biological functioning. The difference in amino acid sequences in both the proteins could be exploited to develop *Pf*LDH specific inhibitors.

Docking

Further, to find out the best molecules that can bind strongly within the active site of the *Pf*LDH, a set of 68 quinolines based molecules were docked in the interface of the protein chain A (active site) of *Pf*LDH, docking results are shown in Table S1. Based on the binding affinity, LE, LLE, and torsion (Table 1), we selected four molecules 3j, 4b, 4h, and 4m, which could be developed as potential antimalarial drugs.

Table 1: Molecules selected on the basis of selectivity for *Pf*LDH in comparison with CQ.

S.No.	Molecules	LLE	LE	Estimated Affinity				Torsion
				pM	nM	μM	mM	
1.	4m							
2.	3j							
3.	4b							
4.	4h							
5.	CQ							

From Figure 1, it is clear that the selected molecules 3j and 4m formed interactions with residues other than the key residue ASP53. The residue ASP53 forms the only H-bond with CQ (reference

inhibitor). Molecules 4b and 4h formed interactions with the key residue ASP53 with some other H-bonds and van der Waal interactions, which shows that selected molecules have significant binding interactions within the active site. In human LDH, CQ forms interaction with ASP51, but our molecules have different interactions than CQ, as shown in Figure 2. So our molecules may have the ability to increase the biological activity to inhibit the glycolytic pathway of the parasite without affecting the host. Moreover, molecules 3j and 4m show a novel mechanism of binding to the active site of *Pf*LDH as both the molecules bind to the residue other than the key binding residue of reference inhibitor CQ. Both the molecules anchors deep into the binding pocket of *Pf*LDH as compared to CQ (Figure 3). The 3-D binding poses of 4b and 4h are shown in Figure S3.

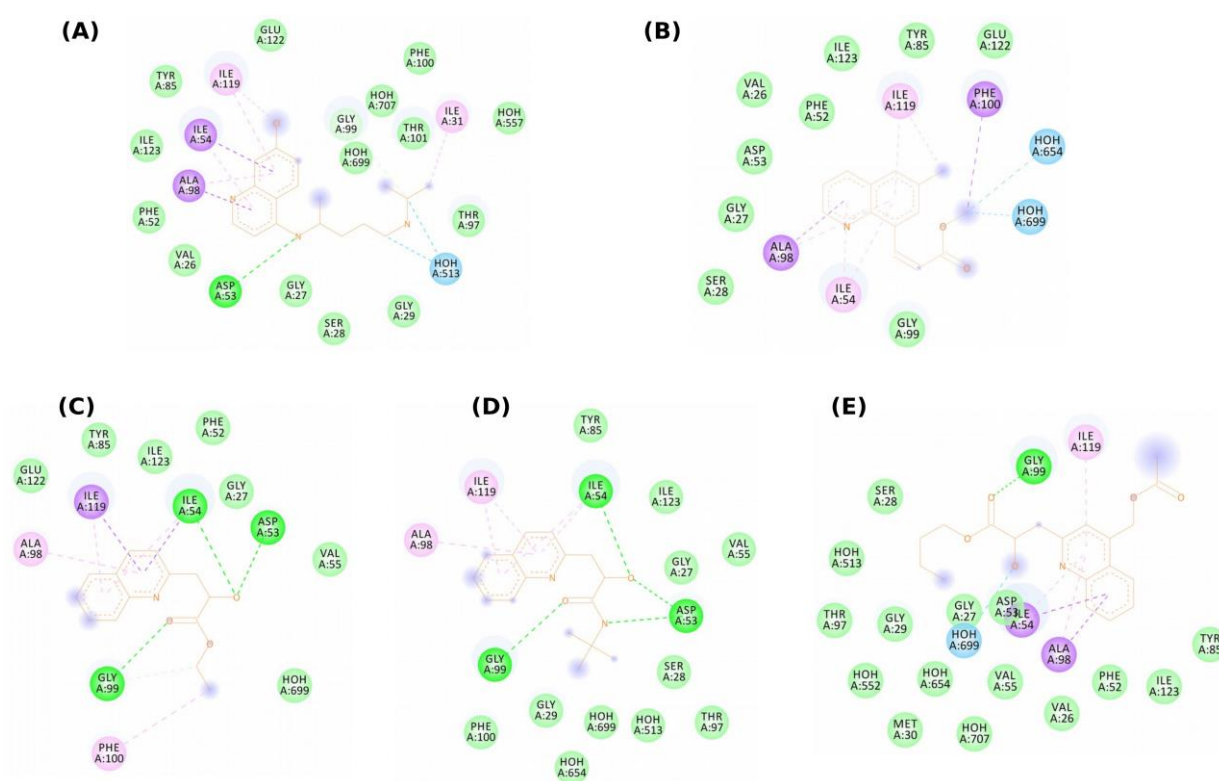


Figure 1: 2D interactions of *Pf*LDH with molecules (A) CQ, (B) 3j, (C) 4b, (D) 4h, (E) 4m.

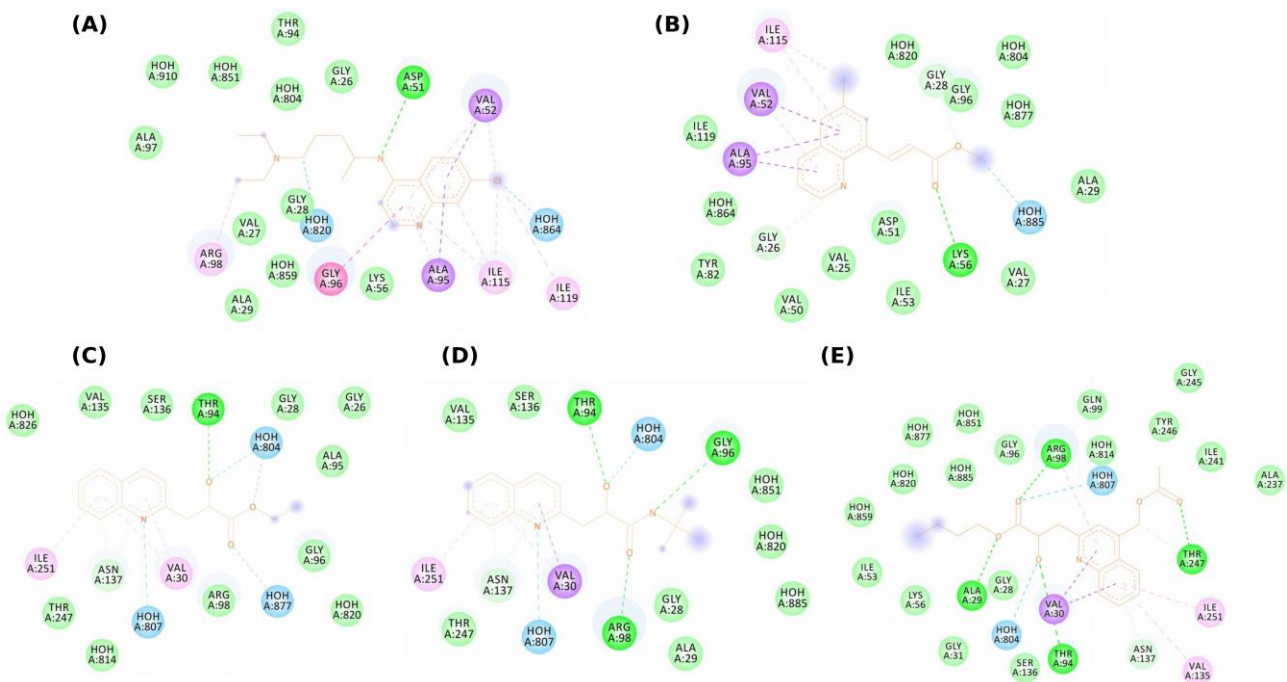


Figure 2: 2D interactions of human LDH with molecules (A) CQ, (B) 3j, (C) 4b, (D) 4h, (E) 4m.

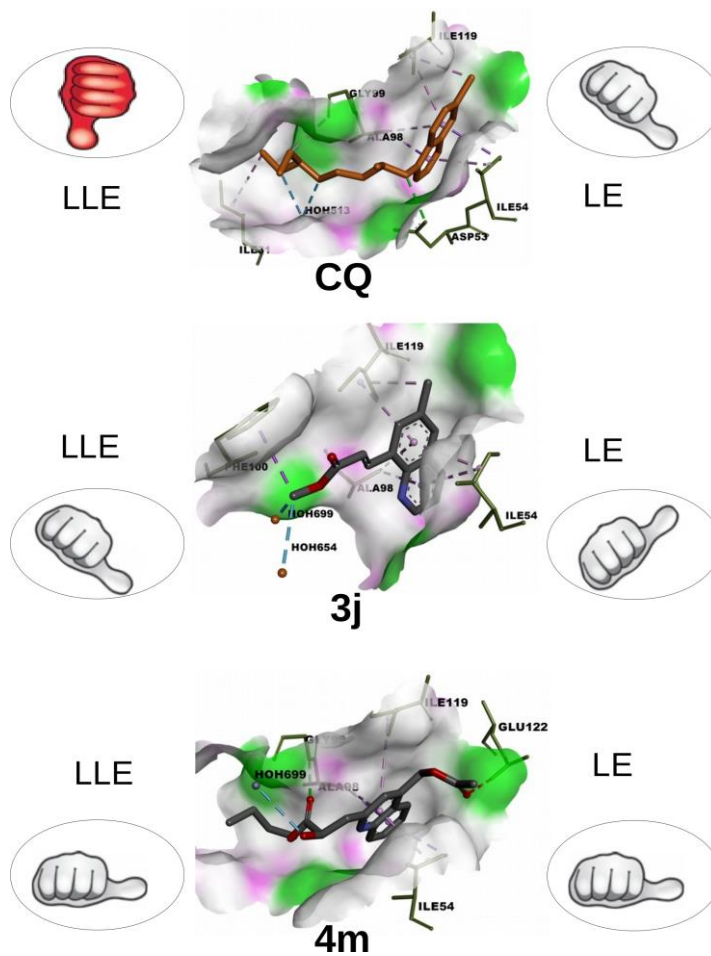


Figure 3: 3D binding poses of *Pf*LDH with molecules CQ, 3j, and 4m.

In order to check the cross-reactivity of selected molecules (3j, 4b, 4h, and 4m) with human LDH, we docked all our 68 molecules with human LDH, and the results are shown in Table S2. All of the selected molecules (3j, 4b, 4h, and 4m) showed poor affinity, LLE, and LE for human LDH. Moreover, the residues of human LDH interacting with CQ are different from those interacting with the selected molecules. Table 2 compares the residues involved in the binding of different molecules to *Pf*LDH and human LDH. The above observations provide the basis for exclusivity to the binding of our molecules (3j, 4b, 4h, and 4m) to *Pf*LDH so that they could be used to inhibit *Pf*LDH without having any effect on human LDH. In order to support our molecular docking results and to provide a rationale for the development of the selected molecules as *Pf*LDH inhibitor, we carried out MD simulations and MM-PBSA analysis.

Table 2: List of interacting amino acid residues of the selected molecules for *Pf*LDH and human LDH proteins.

Molecules	Interacting amino acid residues of <i>Pf</i>LDH-complexes
CQ	ASP53, GLY99 , (ILE31, ILE119*, ILE54*, ALA98*)
3j	(ILE119*, ILE54*, ALA98*, PHE100)
4b	ASP53, GLY99, ILE54, GLY99 , (ILE119*, ILE54*, ALA98, PHE100)
4h	ASP53*, GLY99, ILE54 , (ILE119*, ILE54*, ALA98)
4m	GLY99 , (ILE119, ILE54*, ALA98*)

Molecules	Interacting amino acid residues of human LDH-complexes
CQ	ASP51* , (ILE115**, ILE119, VAL52*, ARG98, GLY96, ALA95*)
3j	LYS56, GLY28, GLY26 , VAL52*, (ALA95*, ILE115*)
4b	THR94, ASN137* , (VAL30*, ILE251)
4h	THR94, GLY96, ARG98, ARG98, ASN137* , (VAL30*, ILE251)
4m	THR94, THR247, ALA29, ARG98, ARG98, THR247* , ASN137, (VAL30*, ILE251, VAL135, ARG98)

Amino acid residues in bold for H-bond.

Amino acid residues mentioned in parenthesis for hydrophobic contacts.

*Two, ** Three number of contacts formed by the particular amino acid residues.

MD simulations and MM-PBSA

MD simulations of the docked complexes alongside the CQ were done for the time duration of 250ns to observe the conformational behavior and stability of the complexes. In addition, the binding free energy of the considerable number of frameworks was figured from the trajectories extracted from the last 3ns. Binding free energy of selected compounds calculated using MM-PBSA calculations [31]. The binding free energy (kJ/mol) (Figure 4) for *Pf*LDH-CQ (-107.192), *Pf*LDH-3j (-161.138), *Pf*LDH-4b (-113.420), *Pf*LDH-4h (-136.928), *Pf*LDH-4m (-194.375) and human LDH-CQ (-79.489), human LDH-3j (-111.752), human LDH-4b (-186.078), human LDH-4h (-169.214), human LDH-4m (-170.515). The binding free energy of CQ has fluctuated more in both the human and *Pf*LDH during the simulation while our selected molecules have produced stable trajectories except molecule 3j in human LDH. The binding free energy consists of Van der Waal interactions, electrostatic, polar solvation, and SASA energy. Contribution of Van der Waal, electrostatic, and SASA energy was negative, whereas positive contributions were shown by polar solvation energy to the overall binding free energy, as shown in Table S3.

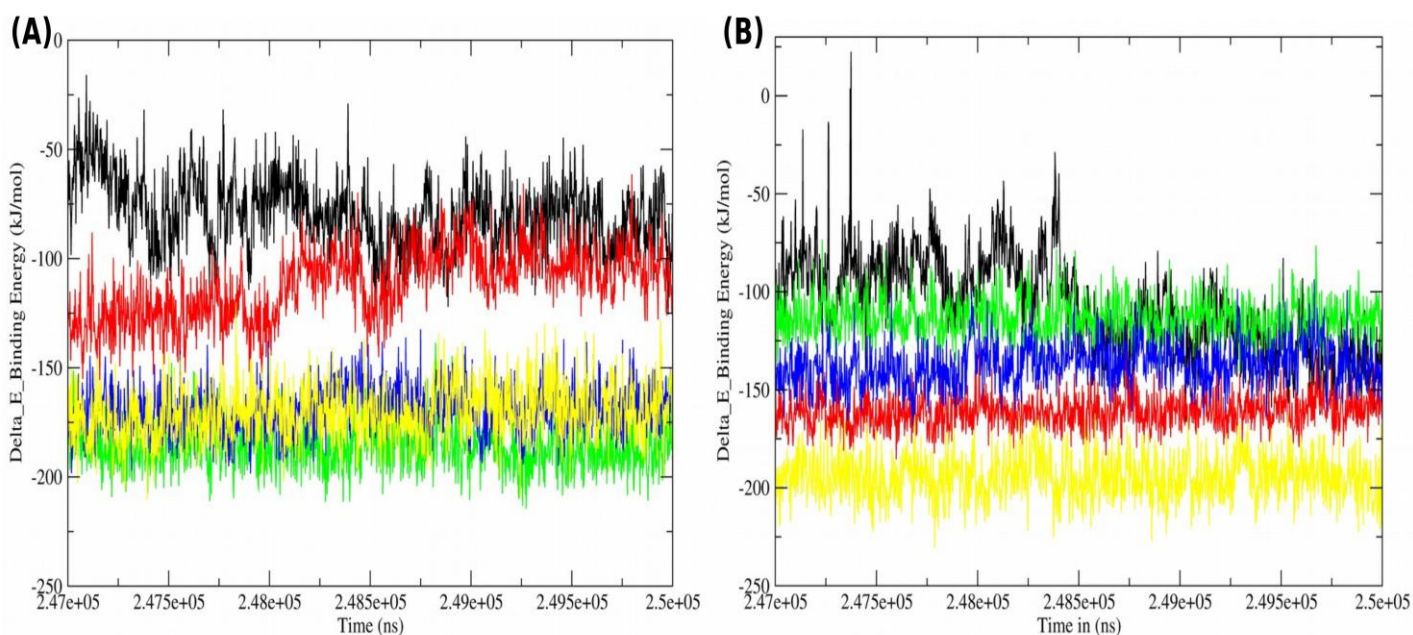


Figure 4: Graphical representation of the Delta_E_Binding free energy kJ/mol showing CQ (black), 3j (red), 4b (green), 4h (blue), 4m (yellow) (A) Human LDH and (B) *Pf*LDH.

To define the selectivity of molecules in comparison with CQ for *Pf*LDH, we calculated the binding free energy ratio with human LDH given in Table 3. According to these findings, we say that the ratio (0.6935) of molecule 3j is best for the development of potential inhibitor against *Pf*LDH in

comparison with the CQ ratio (0.7416). Molecule 4m could also be a potential inhibitor after some changes in chemical structure at a specific group.

The contribution of each residue was also explored (Figure 5), and in *Pf*LDH, major contributing residues for CQ were GLU122 (-28), ASP86 (-25.40), ASP53 (-25.21) while the residues LYS22 (18.10), LYS56 (32.28), LYS118 (23.80), LYS129 (24.29) were weakly contributing. Major contributing residues of molecule 3j were ILE54 (-8.66), ILE119 (-9.78), VAL26 (-5.05), with one weak contributing residue ASP53 (5.59). ILE54 (-6.81), ILE119 (-12.07), VAL26 (-3.02) are highly contributing with one weak contributing residue ASP53 (4.37) in molecule 4b. In molecule 4h ILE54 (-11.88), ILE119 (-8.40), VAL26 (-4.74) are highly contributing residues and ASP53 (13.66) is weak residue. High contributing residues of molecule 4m are MET30 (-6.01), THR101 (-10.82), VAL138 (-5.40). In human LDH GLU54 (-16.30), ASP55 (-18.16), ASP51 (-33.04), GLU103 (-18.90), ASP5 (-11.35), GLU60 (-18.01), ASP81 (-20.84) are highly contributing and LYS56 (18.10), LYS21 (12.62), LYS4 (10.42), ARG98 (21.11), ARG111 (28.63), are weak contributing residues. Major contributing residues of molecule 3j are ILE115 (-6.26), PHE118(-9.93), VAL25 (-4.28). ASN137 (-7.10), VAL135 (-7.51), VAL30 (-4.99) are highly contributing residues in molecule 4b. In molecule 4h ASN137 (-8.11), VAL30 (-4.44) are highly contributing residues. Highly contributing residues of molecule 4m are VAL30 (-5.37), THR94 (-5.57), SER136 (-4.77).

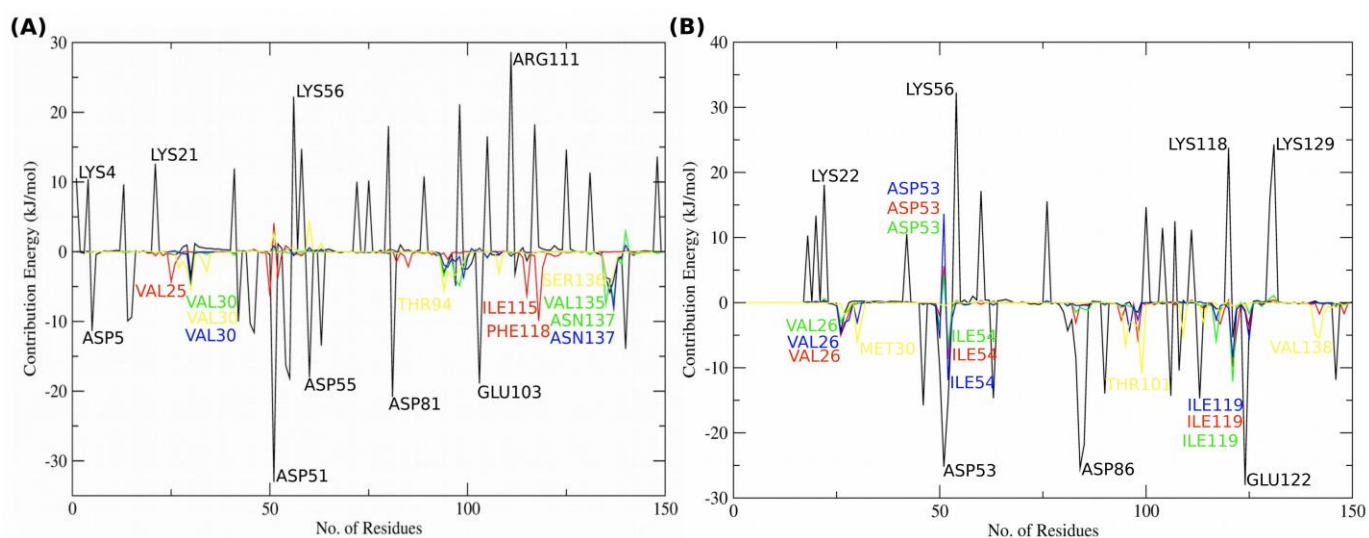


Figure 5: Graphical representation of the MM-PBSA binding energy contribution per residue for CQ (black), 3j (red), 4b (green), 4h (blue), 4m (yellow) (A) Human LDH and (B) *Pf*LDH.

From the above observations, it is clear that the residues contributing to the binding of *Pf*LDH are not showing strong interactions in binding with human LDH. Moreover, the number of residues contributing more favorably to the binding of our molecules to *Pf*LDH are more than residues

involved in binding to human LDH. In addition to it, the residues of all the four selected molecules have performed better than the reference inhibitor CQ in binding to the preferred target *Pf*LDH.

Table 3: Human LDH and *Pf*LDH binding free energy ratio.

Receptors	Binding free energy of molecules with receptors				
	CQ	3j	4b	4h	4m
Human LDH	-79.489	-111.752	-186.078	-169.214	-170.515
<i>Pf</i> LDH	-107.192	-161.138	-113.420	-136.928	-194.375
Ratio	0.7416	0.6935	1.6406	1.2358	0.8772

Conclusion

This research was based on molecular docking, MD simulations, and MM-PBSA approaches to design a new potential inhibitor against *Pf*LDH without affecting the human LDH. Selected molecules 3j and 4m formed interactions with residues other than the key residue ASP53 that provides a novel mechanism of binding at the *Pf*LDH active site. The molecules 4b and 4h formed interactions with key residue ASP53 and they formed H-bonds and van der Waal interactions with other residues, which shows that selected molecules have significant binding interactions within the active site residues than the CQ molecule. In the present work, we found molecule 3j as a potential inhibitor with selectivity for *Pf*LDH, and the chemical structure of molecule 3j may perform as a lead compound for the anti-malarial drug development.

Author contribution statement

RP conceived of and designed the study. RP, RS, and VB analyzed and interpreted the data. RS, VB, and RP critically revised it for important intellectual content. All authors gave final approval of the version to be published.

Acknowledgements

We gratefully acknowledge the CSIR-Institute of Himalayan Bioresource Technology, Palampur for providing the facilities to carry out this work.

Declaration of Competing Interest

None

References :

1. Guerin PJ, Olliaro P, Nosten F, et al (2002) Malaria: Current status of control, diagnosis, treatment, and a proposed agenda for research and development. *Lancet Infect. Dis.*
2. Snow RW, Guerra CA, Noor AM, et al (2005) The global distribution of clinical episodes of *Plasmodium falciparum* malaria. *Nature*. <https://doi.org/10.1038/nature03342>
3. Arrow KJ, Panosian C, Gelband H (2004) Saving Lives, Buying Time: Economics of Malaria Drugs in an Age of Resistance
4. Wellems TE, Plowe C V (2001) Perspective: Chloroquine-Resistant Malaria. *J Infect Dis*
5. Menting JGT, Tilley L, Deady LW, et al (1997) The antimalarial drug, chloroquine, interacts with lactate dehydrogenase from *Plasmodium falciparum*. *Mol Biochem Parasitol*. [https://doi.org/10.1016/S0166-6851\(97\)00095-9](https://doi.org/10.1016/S0166-6851(97)00095-9)
6. Flegg JA, Metcalf CJE, Gharbi M, et al (2013) Trends in antimalarial drug use in Africa. *Am J Trop Med Hyg*. <https://doi.org/10.4269/ajtmh.13-0129>
7. Braga CBE, Martins AC, Cayotopa ADE, et al (2015) Side effects of chloroquine and primaquine and symptom reduction in malaria endemic area (Mâncio lima, Acre, Brazil). *Interdiscip Perspect Infect Dis*. <https://doi.org/10.1155/2015/346853>
8. Fidock DA, Nomura T, Talley AK, et al (2000) Mutations in the *P. falciparum* digestive vacuole transmembrane protein PfCRT and evidence for their role in chloroquine resistance. *Mol Cell*. [https://doi.org/10.1016/S1097-2765\(05\)00077-8](https://doi.org/10.1016/S1097-2765(05)00077-8)
9. Penna-Coutinho J, Cortopassi WA, Oliveira AA, et al (2011) Antimalarial activity of potential inhibitors of *Plasmodium falciparum* lactate dehydrogenase enzyme selected by docking studies. *PLoS One*. <https://doi.org/10.1371/journal.pone.0021237>

10. Waingeh VF, Groves AT, Eberle JA (2013) Binding of Quinoline-Based Inhibitors to *Plasmodium falciparum* Lactate Dehydrogenase: A Molecular Docking Study. *Open J Biophys.* <https://doi.org/10.4236/ojbiphy.2013.34034>
11. Wiwanitkit V (2007) *Plasmodium* and host lactate dehydrogenase molecular function and biological pathways: Implication for antimalarial drug discovery. *Chem Biol Drug Des.* <https://doi.org/10.1111/j.1747-0285.2007.00495.x>
12. Read JA, Wilkinson KW, Tranter R, et al (1999) Chloroquine binds in the cofactor binding site of *Plasmodium falciparum* lactate dehydrogenase. *J Biol Chem.* <https://doi.org/10.1074/jbc.274.15.10213>
13. Egan TJ, Ncokazi KK (2005) Quinoline antimalarials decrease the rate of β -hematin formation. *J Inorg Biochem.* <https://doi.org/10.1016/j.jinorgbio.2005.04.013>
14. Rose PW, Prlić A, Altunkaya A, et al (2017) The RCSB protein data bank: Integrative view of protein, gene and 3D structural information. *Nucleic Acids Res* 45:D271–D281. <https://doi.org/10.1093/nar/gkw1000>
15. Kumar R, Sharma R, Kumar I, et al (2019) Evaluation of Antiplasmodial Potential of C2 and C8 Modified Quinolines: in vitro and in silico Study. *Med Chem* 15:790–800. <https://doi.org/10.2174/1573406414666181015144413>
16. Schneider N, Lange G, Hindle S, et al (2013) A consistent description of Hydrogen bond and DEhydration energies in protein-ligand complexes: Methods behind the HYDE scoring function. *J Comput Aided Mol Des.* <https://doi.org/10.1007/s10822-012-9626-2>
17. Reulecke I, Lange G, Albrecht J, et al (2008) Towards an integrated description of hydrogen bonding and dehydration: Decreasing false positives in virtual screening with the HYDE scoring function. *ChemMedChem.* <https://doi.org/10.1002/cmdc.200700319>
18. ŠAGUD I, ŠKORIĆ I, VUK D, et al (2019) Acetyl- and butyrylcholinesterase inhibitory activity of selected photochemicallysynthesized polycycles. *TURKISH J Chem.* <https://doi.org/10.3906/kim-1903-74>
19. Schärfer C, Schulz-Gasch T, Ehrlich HC, et al (2013) Torsion angle preferences in druglike chemical space: A comprehensive guide. *J Med Chem.* <https://doi.org/10.1021/jm3016816>
20. Abad-Zapatero C, Metz JT (2005) Ligand efficiency indices as guideposts for drug discovery. *Drug Discov. Today*
21. Kuntz ID, Chen K, Sharp KA, Kollman PA (1999) The maximal affinity of ligands. *Proc Natl Acad Sci U S A.* <https://doi.org/10.1073/pnas.96.18.9997>
22. Hopkins AL, Groom CR, Alex A (2004) Ligand efficiency: A useful metric for lead selection. *Drug Discov. Today*

23. BIOVIA DS, Berman HM, Westbrook J, et al (2000) Dassault Systèmes BIOVIA, Discovery Studio Visualizer, v.17.2, San Diego: Dassault Systèmes, 2016. . J Chem Phys. [https://doi.org/10.1016/0021-9991\(74\)90010-2](https://doi.org/10.1016/0021-9991(74)90010-2)
24. Meng EC, Pettersen EF, Couch GS, et al (2006) Tools for integrated sequence-structure analysis with UCSF Chimera. BMC Bioinformatics. <https://doi.org/10.1186/1471-2105-7-339>
25. Abraham M, Van Der Spoel D, Lindahl E, et al (2014) GROMACS User Manual version 5.0.4. www.Gromacs.org. https://doi.org/10.1007/SpringerReference_28001
26. Bhardwaj V, Purohit R (2019) Computational investigation on effect of mutations in PCNA resulting in structural perturbations and inhibition of mismatch repair pathway. J Biomol Struct Dyn. <https://doi.org/10.1080/07391102.2019.1621210>
27. Sharma J, Bhardwaj V, Purohit R (2019) Structural Perturbations due to Mutation (H1047R) in Phosphoinositide-3-kinase (PI3K α) and Its Involvement in Oncogenesis: An in Silico Insight. ACS Omega. <https://doi.org/10.1021/acsomega.9b01439>
28. Schüttelkopf AW, Van Aalten DMF (2004) PRODRG: A tool for high-throughput crystallography of protein-ligand complexes. Acta Crystallogr Sect D Biol Crystallogr. <https://doi.org/10.1107/S0907444904011679>
29. Kumari R, Kumar R, Lynn A, A. L (2014) g_mmpbsa-a GROMACS tool for high-throughput MM-PBSA calculations. J Chem Inf Model 54:1951. <https://doi.org/10.1021/ci500020m>
30. Kollman PA, Massova I, Reyes C, et al (2000) Calculating structures and free energies of complex molecules: Combining molecular mechanics and continuum models. Acc Chem Res. <https://doi.org/10.1021/ar000033j>
31. Massova I, Kollman PA (2000) Combined molecular mechanical and continuum solvent approach (MM- PBSA/GBSA) to predict ligand binding. Perspect. Drug Discov. Des